# Effect of PEKK oligomers sizing on the dynamic mechanical behavior of poly(ether ketone ketone)/carbon fiber composites

**Mike Abidine Alexandre,[1,2,3†] Eric Dantras,[2] Colette Lacabanne,[2] Emile Perez,[3] Sophie Franceschi,[3] Damien Coudeyre[1]**

[1]Institut de Recherche Technologique (IRT) Saint Exupéry, B612 Building, 3 Rue Tarfaya, CS34436, 31405, Toulouse Cedex 4, France

[2]Centre Interuniversitaire de Recherche et d'Ingénierie des Matériaux (CIRIMAT), Physique des Polymères, Université de Toulouse, 31 062, Toulouse Cedex 09, France

[3]Laboratoire des Interactions Moléculaires Réactivité Chimique et Photochimique (IMRCP), Université de Toulouse, 31 062, Toulouse Cedex 09, France

Correspondence to: E. Dantras (E-mail: eric.dantras@univ-tlse3.fr)

**ABSTRACT:** Poly(ether ketone ketone) (PEKK)/unidirectional carbon fiber (CF) composites have a poor interface. Accordingly, PEKK oligomer (PEKKo) sizing with a chemical compatibility with PEKK is proposed for promoting interfacial interactions in order to enhance mechanical performances. The thermal stability until 500 °C has been shown by thermogravimetric analysis (TGA). In order to compare static and dynamic sizing methods, "lab sizing" and "pilot sizing" were carried out. Scanning electron microscopy images of freeze fractures of PEKK/unsized CF, PEKK/PEKKo lab-sized CF and PEKK/PEKKo pilot-sized CF show that the PEKKo sizing causes an improvement of fiber/PEKK interactions, regardless of the sizing method. Indeed, in both cases, there is a continuity of matter at the interface while we observe a poor wetting of CF by matrix in PEKK/unsized CF. Dynamic mechanical relaxations in shear were analyzed as a function of temperature. The increase of storage modulus upon sizing is observed for both methods but it is more important for PEKKo pilot sizing. In the same way, the mechanical energy loss increases, it reflects the optimization of stress transfer between matrix and fibers.

**KEYWORDS:** composites; mechanical properties; structure–property relationships; thermoplastics

**DOI: 10.1002/app.48818**

## INTRODUCTION

Sizing and surface modifications of carbon fibers (CFs) for matrix reinforcement in composites are under numerous investigations namely for preparation[1–8] and also for their influence on mechanical interface.[9–17] Gargano *et al.* showed significant influence of sizing during a high shock wave impulse on polymer/CF laminates. An agent with high chemical compatibility with the polymer matrix promotes strong bonding and improves blast properties of laminates.[18] High temperature thermoplastic matrix composites reinforced with continuous CFs[19,20] are interesting for impact behavior and damage tolerance.[21] Additionally, it makes possible to envisage the use of recyclable structural composites[22–25] with potential applications in aeronautics and space domains. The poly(ether ketone ketone) (PEKK) matrices, with their different configurations, occupy a privileged position among the poly(aryl ether ketone) (PAEK) family.[26] The handling of continuous CF requires the presence of sizing which is also necessary for the stress transfer at the fiber/matrix interface in composites. The development of PEKK/CF composites therefore involves the availability of a thermostable sizing compatible with PEKK. Due to a poor thermal stability, thermoset sizing would undergo a degradation during implementation of composites[27]; moreover, they are not chemically compatible with PAEK. The work of Giraud *et al.*[28,29] identified two sizing agents that fulfill both requirements: the poly(ether imide) (PEI)[30] for its high miscibility[31–34] with PAEK matrix and the PEKK oligomers (PEKKo)[29] for their chemical analogy. For aeronautical applications, the inconvenience of PEI is its solubility in skydrol and kerosene.[35,36] Consequently, PEKKo is a most relevant solution to explore. Moreover, the influence on fracture mechanisms of

†Present address: Centre de Recherche sur les Ions, les Matériaux et la Photonique, Université de Caen, IUT Grand Ouest Normandie, Pôle d'Alençon, 61 250 Damigny, France.

new thermoplastic sizing in PEKK/CF composites[37] was also observed. The aim of this study was to investigate the influence of sizing on the composite behavior in its linear domain of strain. Accordingly, a study by dynamic mechanical analysis (DMA) was carried out. Different PEKK/CF samples with and without sizing were processed and analyzed in a comparative way to highlight the effect of sizing. Two sizing methods were carried out in order to explore the influence of sizing rates: the "lab sizing," with a higher rate, was performed at CIRIMAT; the "pilot sizing" with a lower rate was carried out on the pilot line developed by IRT Saint-Exupéry.

## EXPERIMENTAL

### Materials

PEKK matrix, KEPSTAN 7003 synthesized by Arkema (France) in the form of powder with a granulometry of 20 μm, was used for this work. The fibrous reinforcement, AS4 12000 unsized filaments, provided by Hexcel was used. The sizing agent was PEKK oligomers provided by Arkema with a Terephthalic/Isophthalic configuration 20/80. A sizing formulation with a concentration in PEKK oligomers of 0.5 wt % was elaborated by the sonofragmentation-dispersion process.[38] Thanks to this procedure, PEKKo particles of 5 μm were obtained.

The thermal stability of PEKKo sizing formulations was controlled by TGA. Figure 1(a,b) shows the weight loss and the derivative weight loss thermograms respectively. It is clear that formulation auxiliaries are totally degraded at 360 °C, that is, the drying temperature of sizing process. The degradation temperature of PEKKo was observed at 500 °C: this temperature is higher than the implementation temperature of PEKK/CF composites so that PEKKo remains stable during the implementation process.

### Sizing Preparation

**Laboratory Process.** Lab-sized CFs were prepared by static immersion in PEKKo aqueous dispersion at 0.5 wt % and dried at 360 °C during 1 min. The sizing rate as controlled by weighting was 10.5 wt % of CF.

**Pilot Process.** Pilot-sized CFs were prepared by the dynamic immersion in PEKKo aqueous dispersion at 0.5 wt % with a sizing speed of 8 m $min^{-1}$ and dried at 360 °C in an IF oven. The sizing rate as controlled by weighting was 2.2 wt % of CF.

### PEKK/CF Composite Processing

Figure 2 shows a schematic illustration of the processing setup. PEKK/CF composites were prepared by impregnation of unidirectional CFs with PEKK dispersion in ethanol solvent (1), dried at 360 °C during 1 min (2) and placed in an aluminum mold at 360 °C during 15 min under low pressure (<20 MPa) (3). The aluminum mold was cooled at ambient temperature (4). The dimensions of the composite samples were 90 mm long × 10 mm wide × 0.5–0.6 mm thick (5). The fiber content of composites was between 14 and 16 wt %.

### Methods

**Scanning Electron Microscopy.** All samples were examined with a scanning electron microscope (SEM) in backscattered electrons, on JEOL JSM 7800 Prime microscope with an acceleration of 10 kV, a magnification of ×5.000 and a working distance of 15.0 mm.

**Dynamic Mechanical Analysis.** The DMA were performed with the Advanced Rheometric Expansion System strain-controlled rheometer (ARES G2) of TA Instruments in the torsion rectangular mode at an angular frequency of 1 rad $s^{-1}$. The storage shear modulus ($G'$) and loss shear modulus ($G''$) were recorded as a function of temperature between −125 and 270 °C at a scanning rate of 3 °C $min^{-1}$. Measurements were realized in the linear zone under a strain $\gamma = 0.1\%$. The dimension of samples was 40 mm long, 10 mm wide, and between 500 and 600 μm thick.

## RESULTS AND DISCUSSION

### Observation of Fracture Surfaces

Freeze fractures at LNT of PEKK/unsized CF, PEKK/PEKKo lab-sized CF, and PEKK/PEKKo pilot-sized CF composites were observed by SEM in order to determine the influence of the PEKKo sizing. This first approach allows us to perform a qualitative comparison of the matrix/fiber interface. Figure 3

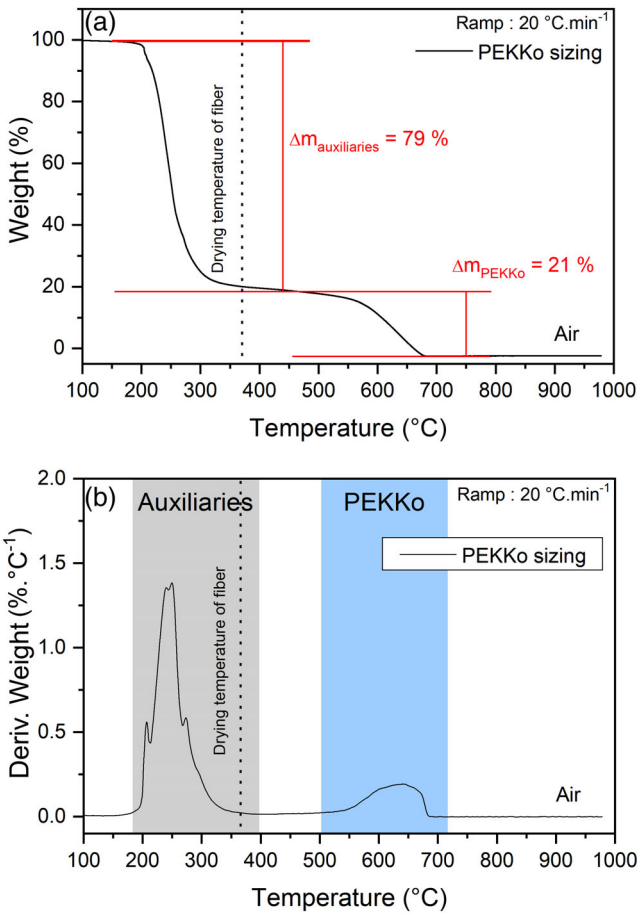


**Figure 1.** TGA thermograms of the PEKKo sizing formulation under air, with a ramp of 20 °C $min^{-1}$. (a) Weight loss as a function of temperature. (b) Derivative weight loss as a function of temperature. [Color figure can be viewed at wileyonlinelibrary.com]

(a) presents the freeze fracture of the unsized CF composite. There is a discontinuity between CF and polymer matrix which reveals a poor wetting of CF by the matrix in composites with unsized fibers.

Figure 3(b,c) presents freeze fractures of the PEKK/PEKKo lab-sized CF and the PEKK/ PEKKo pilot-sized CF composites, respectively. In both cases, we observe a continuity of matter at the interface. There is a more important wetting of CF by matrix so that we might expect a better transfer of stress between CF and polymer matrix. Moreover, it is important to note that there is no degradation during the composite processing.

### Dynamic Mechanical Relaxation

**Composite with Unsized CF.** Figure 4 represents the storage modulus ($G'$) as a function of temperature: blue circles (○) correspond to the unsized CF composite and black squares (□) are for the PEKK matrix. In the whole temperature range, the storage modulus of the unsized composite is of course higher than the one of the PEKK matrix. In the vitreous domain, $G'$ of the PEKK matrix is multiplied by 2 in the unsized composite. This improvement is due to the reinforcement of the vitreous matrix by CFs. In the rubbery domain, $G'$ of the unsized composite is six times higher than the one of the PEKK matrix; this increase is due to the contribution of the topological entanglements that creates physical nods. Phenomenologically, they play the role of dynamic crosslinks. The $\Delta G$ step is defined by eq. (1):

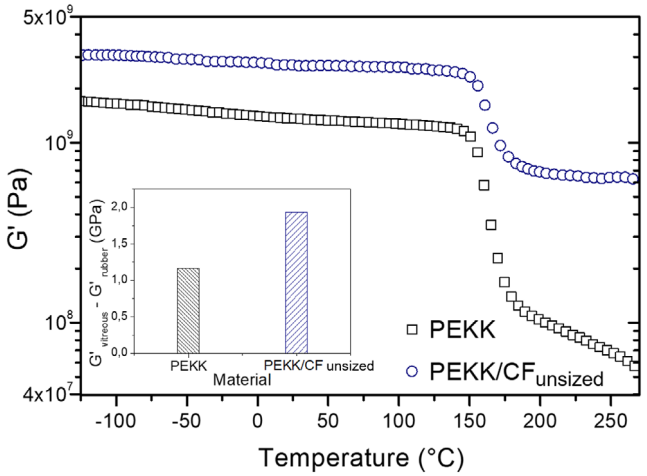


**Figure 4.** Storage modulus $G'$ as a function of temperature for the PEKK/unsized CF composite (○) and the PEKK matrix (□). The framed detail represents the viscoelastic step of the storage modulus for both materials. [Color figure can be viewed at wileyonlinelibrary.com]

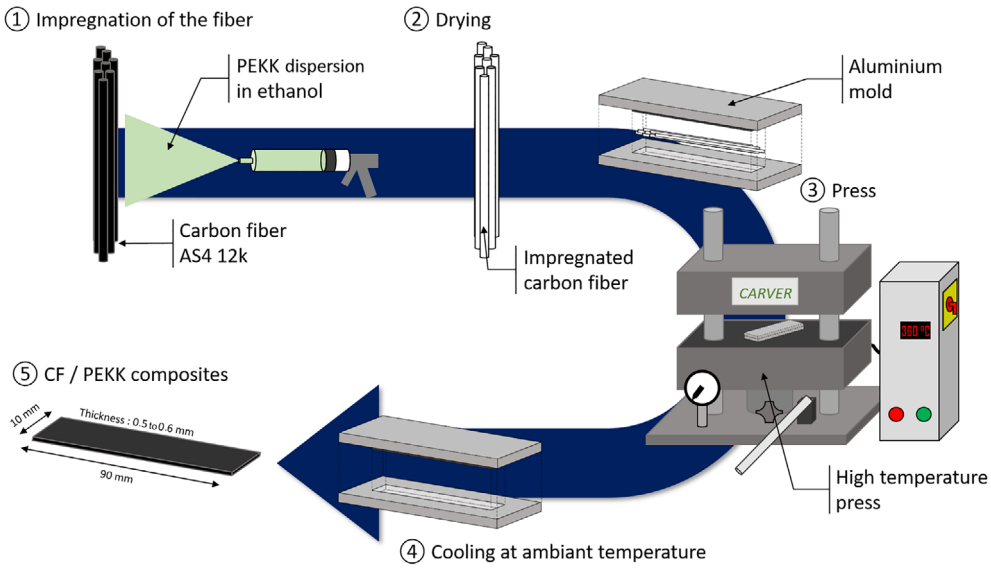


**Figure 2.** Schematic illustration of the preparation of CF/PEKK composites. [Color figure can be viewed at wileyonlinelibrary.com]

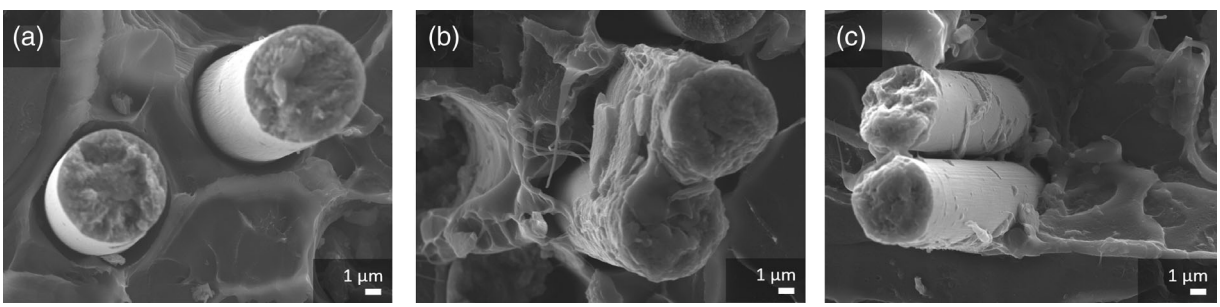


**Figure 3.** Freeze facture of the (a) PEKK/unsized CF composite, (b) PEKK/PEKKo lab-sized CF composite, and (c) PEKK/PEKKo pilot-sized CF composite.

$$\Delta G = G'_{\text{vitrious}}(100\ ^\circ\text{C}) - G'_{\text{rubbery}}(200\ ^\circ\text{C}) \quad (1)$$

The histogram (framed detail of Figure 4) represents the step of the $G'$ modulus associated with the viscoelastic transition ($\Delta G$) as a function of the material.

The increase of $\Delta G$ ($\Gamma_{\Delta G}$) is defined by eq. (2):

$$\Gamma_{\Delta G} = \frac{\Delta G_{\text{unsized composite}} - \Delta G_{\text{PEKK matrix}}}{\Delta G_{\text{PEKK matrix}}} \quad (2)$$

$\Gamma_{\Delta G}$ for the unsized composite is 66%. Note that, above 200 °C, PEKK exhibits an irreversible flow despite its semicrystalline structure. This flow is no more observed in composites.

Figure 5 represents the loss modulus ($G''$) as a function of temperature for the unsized composite (○), and the PEKK matrix (□). The peak at higher temperature (162 °C) is referred as the α relaxation; it is due to the viscoelastic transition. The reinforcement by CF does not modify the $T_\alpha$ maximum temperature of the α relaxation. The histogram (framed detail on Figure 3) represents the area of the α relaxation peak measured between 100 and 210 °C, as a function of the material. We observe an increase of 27% for the unsized composite compared to the matrix. This energy loss mechanism involves a stick–slip effect.[21,39–41] This effect which is present in a wide range of composites, indicates a specific dissipative energy due to the creation and disruption of physical bonds between the matrix and the fibrous reinforcement.

Figure 6 represents tan δ as a function of temperature for the unsized composite (○), and the PEKK matrix (□). The histogram (framed detail on Figure 6) reports the area of the α relaxation peak determined between130 and 205 °C, for tan δ as a function of the material. We observe a decrease of 54% for the unsized composite compared to the matrix.

At $T_\alpha$ (162 °C), tan δ of the PEKK matrix is $2.77 \times 10^{-1}$ compared to $1.40 \times 10^{-1}$ for the unsized composite. Tan δ is defined as the ratio between $G''/G'$. At $T_\alpha$, $G''$ has the same order of magnitude for the PEKK matrix and the unsized composite. Accordingly, tan δ is led by $G'$ which is much higher for the unsized CF composite than for the PEKK matrix.

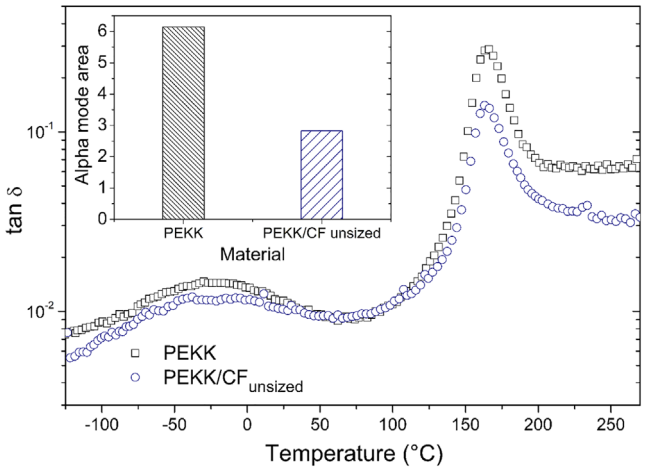


**Figure 6.** Tan δ as a function of temperature for the PEKK/unsized CF composite (○) and the PEKK matrix (□). The framed detail represents the area of the α relaxation peak of tan δ for both materials. [Color figure can be viewed at wileyonlinelibrary.com]

**Composite with PEKK Oligomer Lab-Sized CF.** Figure 7 represents the storage modulus $G'$ as a function of temperature for the PEKKo lab-sized composite (green inverted triangles ▽), and for the unsized composite (blue circles ○). In the whole temperature range, $G'$ of the PEKKo lab-sized composite is higher than $G'$ of the unsized composite. In the vitreous domain, $G'$ of PEKKo lab-sized composite is multiplied by 1.2: This improvement is due to a higher efficiency of the CF reinforcement of the vitreous matrix due to the PEKKo lab sizing. In the rubbery domain, $G'$ of the PEKKo lab-sized composite is 1.7 times the one of the unsized

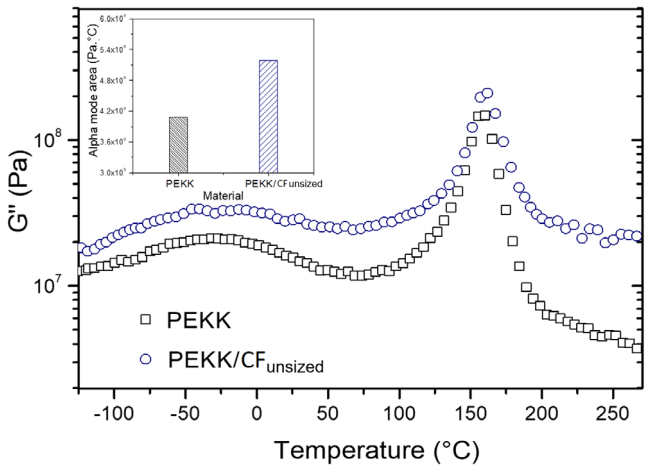


**Figure 5.** Loss modulus $G''$ as a function of temperature for the PEKK/unsized CF composite (○) and the PEKK matrix (□). The framed detail represents the area of the α relaxation peak for both materials. [Color figure can be viewed at wileyonlinelibrary.com]

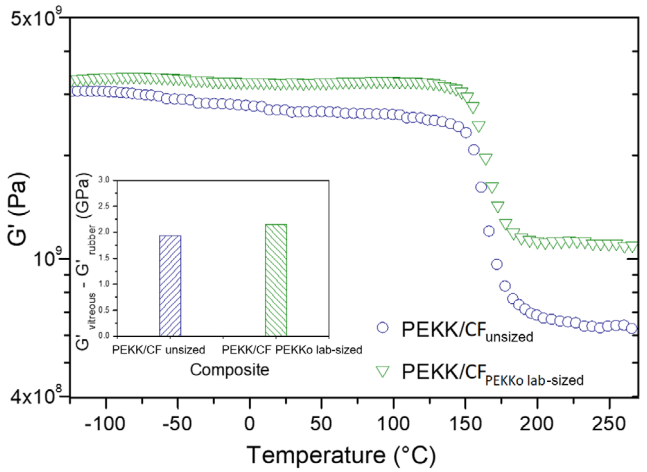


**Figure 7.** Storage modulus $G'$ as a function of temperature for the PEKK/PEKKo lab-sized CF composite (▽) and the PEKK/unsized CF composite (○). The framed detail represents the viscoelastic step of the storage modulus for both materials. [Color figure can be viewed at wileyonlinelibrary.com]

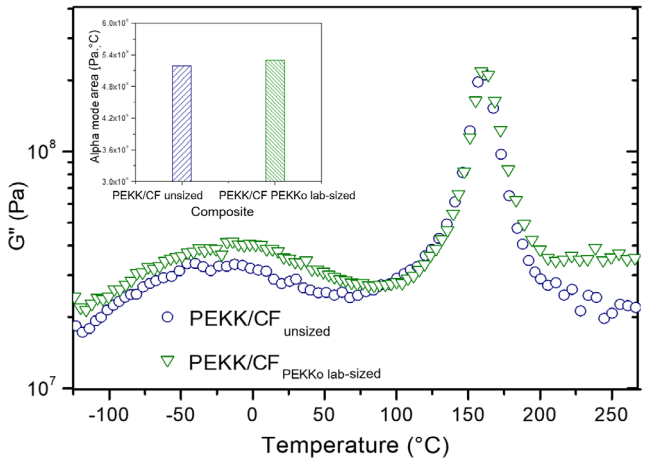


**Figure 8.** Loss modulus $G''$ as a function of temperature for the PEKK/PEKKo lab-sized CF (▽) and the PEKK/unsized CF composite (○). The framed detail represents the area of the α relaxation peak for both composites. [Color figure can be viewed at wileyonlinelibrary.com]

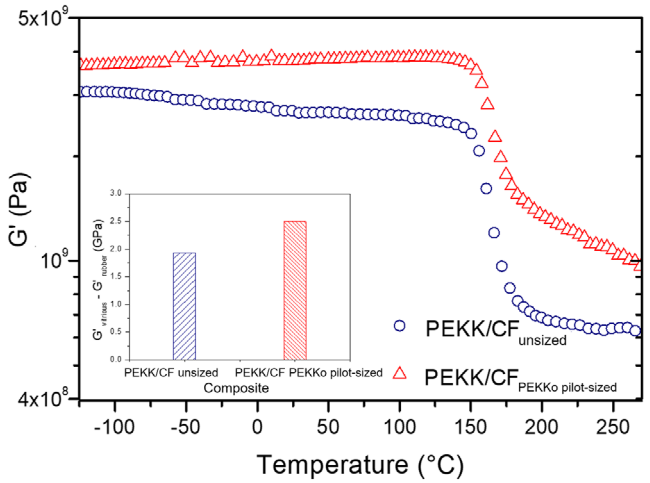


**Figure 10.** Storage modulus $G'$ as a function of temperature for the PEKK/PEKKo pilot-sized CF composite (△) and the PEKK/unsized CF composite (○). The framed detail represents the viscoelastic step of the storage modulus for both composites. [Color figure can be viewed at wileyonlinelibrary.com]

composite due to the contribution of the PEKKo lab sizing to the topological entanglements. Then, physical modes acting as cross-links are favored. The histogram (framed detail of Figure 7) represents $\Delta G$ as a function of the various composites. Taking as reference the unsized CF composites, the gain of $\Delta G$ for the PEKKo lab-sized CF composite is 11%.

The thermogram (Figure 8) represents the $G''$ energy loss as a function of temperature for the PEKK/PEKKo lab-sized CF composite (▽) and for the PEKK/unsized CF composite (○). We observe that the α relaxation position is not modified by the presence of PEKKo sizing. The histogram of Figure 6 represents the area associated with the α mode determined between 100 and 210 °C as a function of the composite. We observe for the α mode area associated with the PEKKo lab-sized composite, an increase slightly higher than the one of the PEKK/unsized CF composite. We conclude that dissipative effects at the CF/PEKKo lab-sized/PEKK interface reflect a mild enhancement of the stick–slip effect observed *in* unsized composite.

Figure 9 represents the tan δ as a function of temperature for the PEKKo lab-sized CF composite (▽), and the unsized composite (○). At $T_\alpha$ (162 °C), tan δ of the unsized composite is $1.40 \times 10^{-1}$ compared to $1.07 \times 10^{-1}$ for the PEKKo lab-sized CF composite. $G''$ between the unsized composite and the PEKKo lab-sized CF composite at $T_\alpha$ is of the same order of magnitude. Then, tan δ is led by $G'$. $G'$ (unsized composite) is inferior to $G'$ (PEKKo lab-sized CF composite) hence tan δ (unsized composite) is superior to tan δ (PEKKo lab-sized CF composite) as shown by Figure 7. The decrease of tan δ due to the influence of sizing is another view of the influence of CF reinforcement of the vitreous matrix. The histogram (framed

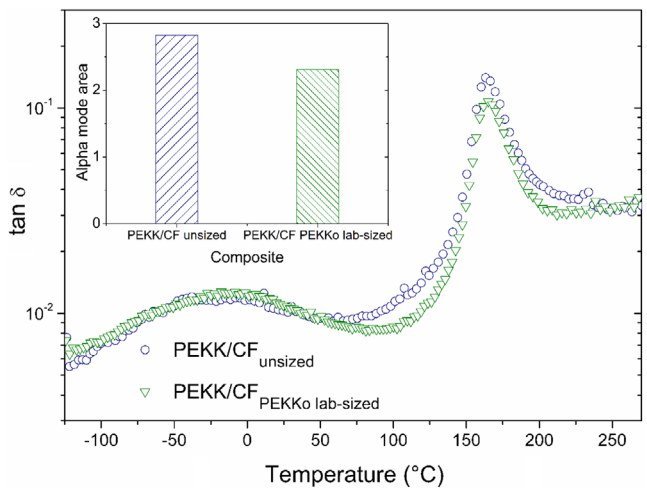


**Figure 9.** Tan δ as a function of temperature for the PEKK/PEKKo lab-sized CF composite (▽) and the PEKK/unsized CF composite (○). The framed detail represents the area of the α relaxation peak of tan δ for both composites. [Color figure can be viewed at wileyonlinelibrary.com]

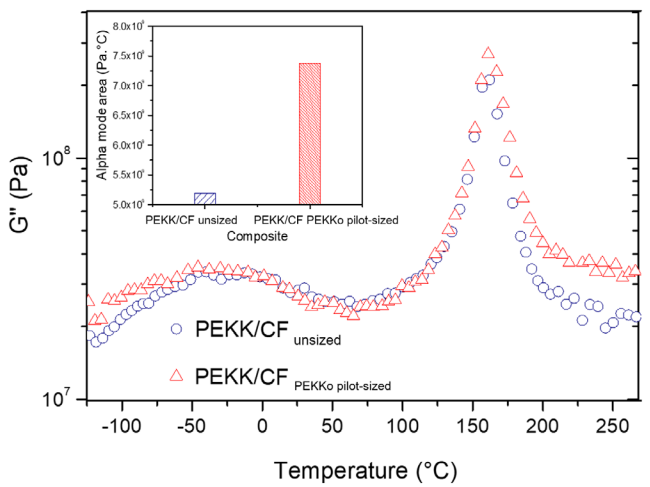


**Figure 11.** Loss modulus $G''$ as a function of temperature for the PEKK/CF PEKKo pilot-sized composite (△) and for PEKK/CF unsized composite (○). The framed detail represents the area of the α relaxation peak for both composites. [Color figure can be viewed at wileyonlinelibrary.com]

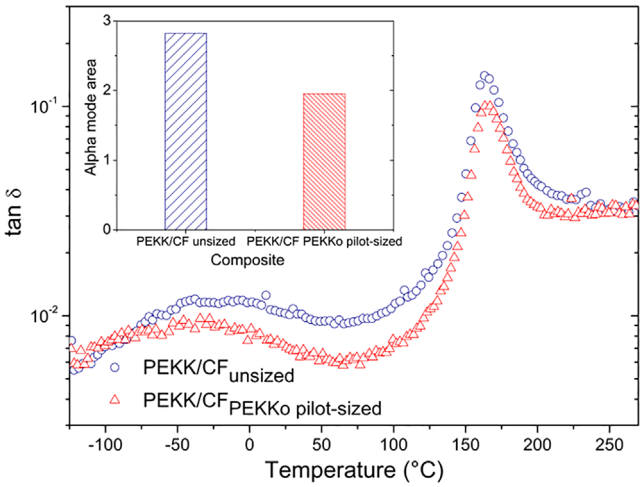


**Figure 12.** Tan δ as a function of temperature for the PEKK/CF PEKKo pilot-sized composite (△) and for PEKK/CF unsized composite (○). The framed detail represents the area of the α relaxation peak of tan δ for both composites. [Color figure can be viewed at wileyonlinelibrary.com]

detail on Figure 9) represents the area of the α relaxation peak of tan δ measured between 130 and 205 °C as a function of the composite. It is recorded a decrease of 18% for lab-sized CF composite compared to the unsized composite.

**Composite with PEKK Oligomer Pilot-Sized CF.** Figure 10 represents the $G'$ storage modulus as a function of temperature for the PEKK/PEKKo pilot-sized CF composite (red triangles △), and for the unsized composite (blue circles ○) used as reference. In the whole temperature range, $G'$ for the PEKK/PEKKo pilot-sized CF composite is higher than for the PEKK/unsized CF composite. In the vitreous domain, the $G'$ of PEKK/PEKKo pilot-sized CF composite is 1.5 times higher than the one of unsized composite this enhancement is due a strengthening of the vitreous matrix by the PEKKo pilot sizing. In the rubbery domain, $G'$ of PEKK/PEKKo pilot-sized CF composite is two times higher than the one of unsized composite; this effect reflects the contribution of PEKKo pilot sizing to topological entanglements creating physical nods. The histogram on Figure 8 represents $\Delta G$ for both composites. Taking as reference the PEKK/unsized CF composite, the gain of $\Delta G$ for the PEKK/PEKKo pilot-sized CF composite is 29%.

Figure 11 represents the $G''$ energy loss as a function of temperature for the PEKKo pilot-sized composite (△), and for the unsized composite (○). The α relaxation is not modified by the use of PEKKo pilot sizing. The histogram (framed detail of Figure 9) represents the area associated with the α relaxation mode determined between 100 and 210 °C for both composites. We observe a gain of 42% for the α mode area associated with the pilot-sized composite compared to the unsized composite. We conclude that the dissipative effect of stick–slip observed in composite with unsized fibers is strongly favored by the presence of the PEKKo pilot sizing. This result is consistent with SEM images showing a wetting of CF by the matrix in composite with PEKKo pilot sizing.

Figure 12 represents tan δ as a function of temperature for the PEKKo pilot-sized composite (△), and the unsized composite (○). At $T_\alpha$ (162 °C), tan δ of unsized composite is $1.40 \times 10^{-1}$ compared to $0.97 \times 10^{-1}$ for the PEKKo pilot-sized composite. Both $G'$ and $G''$ between the unsized composite and the PEKKo pilot-sized composite are varying. Since the major variation is due to $G'$, a decrease of tan δ is observed. The histogram (framed detail on Figure 12) represents the area of the α relaxation peak determined between 130 and 205 °C as a function of the composite. We observe a decrease of 31% for PEKKo pilot-sized composite compared to the unsized composite.

We observe a difference between tan δ for sized composites of $0.1 \times 10^{-1}$ and $1.07 \times 10^{-1}$ for PEKKo lab sized and $0.97 \times 10^{-1}$ for PEKKo pilot sized. This demonstrates once again the relevance of low sizing rates favoring stick–slip effects and CF/matrix cohesion (Figure 13).

Figure 13 shows a schematic representation of composites with PEKKo lab sizing and PEKKo pilot sizing. For higher sizing rate

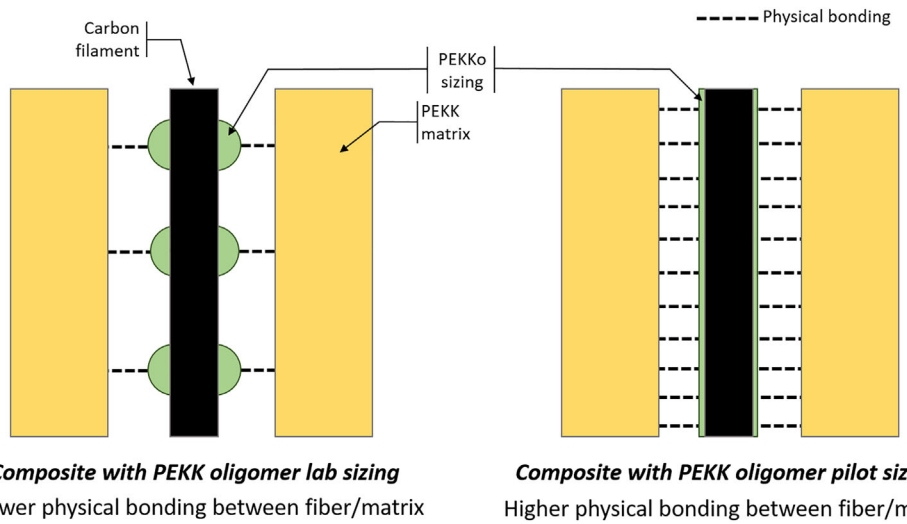


**Figure 13.** Schematic illustration of fiber/matrix interface for PEKK/PEKKo sized CF composites for lab sizing and pilot sizing. [Color figure can be viewed at wileyonlinelibrary.com]

(lab sizing), sizing is deposited as droplets: for lower sizing rate (pilot sizing), the sizing speeds onto CFs. The increase of stick–slip effects for PEKKo pilot-sized composite can be explained by a homogenous sizing deposit which favors higher density of physical bonding at the fiber/matrix interface.

## CONCLUSIONS

This study is focused on the effect of PEKKo sizing on PEKK/CF composites. The SEM images of freeze fractures demonstrate an evident continuity of matter at the PEKK/CF interfaces in both PEKK/PEKKo lab-sized CF and PEKK/PEKKo pilot-sized CF composites. Accordingly, PEKK/CF interactions are favored in both cases, that is, the major interest of a sizing with a chemical compatibility with the matrix, like PEKK oligomers.

DMAs in shear are well suited to analyze the effect of interfaces on the dynamic mechanical performances of composites. The increase of the storage modulus upon the introduction of sizing is observed in both PEKK/PEKKo lab-sized CF and PEKK/PEKKo pilot-sized CF composites. It is interesting to note that this last one is more important for the PEKKo pilot sizing. In the same way, we observe a more important increase of the energy loss indicating the optimization of stress transfer at the interface for the PEKK/PEKKo pilot-sized composite. This effect is due to the spread of the sizing on the fiber due to the low sizing rate. Then, the stick–slip at the fiber/matrix interfaces is evidently favored. It is interesting to note that the decrease of tan δ upon PEKKo sizing, reflect that the predominant effect is the increase of the glassy modulus.

## ACKNOWLEDGMENTS

The results of this study were obtained in the context of the research project "COMPINNOVTP" at the IRT Saint Exupéry. The authors thank the industrial and academic members of the IRT who supported this project through their contributions, both financial and in terms of specific knowledge: Industrial members: AIRBUS OPERATIONS, ARIANE GROUP, AIRBUS GROUP INNOVATIONS, AIRBUS HELICOPTERS, and THALES ALENIA SPACE. Academic members: CIRIMAT, CNRS, ICA, IMRCP, ISAE, and UPS. The authors would also like to thank the "Commissariat Général aux Investissements" and the "Agence Nationale de la Recherche" for their financial support in the framework of the "Programme d'Investissement d'Avenir" (PIA). We thank the Arkema group for providing PEKK oligomers.

## REFERENCES

1. Ogawa, H., Shima, M. U.S. Pat. 4,420,512 (**1983**).
2. Bergerat, J.-M., Giraud, I., Dantras, E., Perez, E., Lacabanne, C. U.S. Pat. 2011/0300381 A1 (**2011**).
3. Liu, J.; Ge, H.; Chen, J.; Wang, D.; Liu, H. *J. Appl. Polym. Sci.* **2012**, *124*, 864.
4. Lee, W.; Lee, J. U.; Cha, H.; Byun, J. *RSC Adv.* **2013**, *3*, 25609.
5. Zhang, R. L.; Liu, Y.; Huang, Y. D.; Liu, L. *Appl. Surf. Sci.* **2013**, *287*, 423.
6. Zhang, S.; Liu, W. B.; Hao, L. F.; Jiao, W. C.; Yang, F.; Wang, R. G. *Compos. Sci. Technol.* **2013**, *88*, 120.
7. Zhang, T.; Zhao, Y.; Li, H.; Zhang, B. *J. Appl. Polym. Sci.* **2018**, *135*, 46111.
8. Zhang, M.; Li, M.; Liu, L.; Fu, J.; Jin, L.; Shang, L.; Xiao, L.; Ao, Y. *Polym. Compos.* **2018**, *40*, E744.
9. Tang, L.-G.; Kardos, J. L. *Polym. Compos.* **1997**, *18*, 100.
10. Zhao, Y.; Duan, Y.; Xiao, H. *J. Mater. Eng.* **2007**, *S1*, 121.
11. Zhang, R. L.; Huang, Y. D.; Liu, L.; Tang, Y. R.; Su, D.; Xu, L. W. *Appl. Surf. Sci.* **2011**, *257*, 1840.
12. Dai, Z.; Shi, F.; Zhang, B.; Li, M.; Zhang, Z. *Appl. Surf. Sci.* **2011**, *257*, 6980.
13. Zhang, X.; Fan, X.; Yan, C.; Li, H.; Zhu, Y.; Li, X.; Yu, L. *ACS Appl. Mater. Interfaces*. **2012**, *4*, 1543.
14. Li, M.; Gu, Y.; Liu, Y.; Li, Y.; Zhang, Z. *Carbon*. **2013**, *52*, 109.
15. Zhao, Z.; Du, S.; Li, F.; Xiao, H.; Li, Y.; Zhang, W.; Hu, N.; Fu, S.-Y. *Compos. Commun.* **2018**, *8*, 1.
16. Moosburger-Will, J.; Bauer, M.; Laukmanis, E.; Horny, R.; Wetjen, D.; Manske, T.; Schmidt-Stein, F.; Töpker, J.; Horn, S. *Appl. Surf. Sci.* **2018**, *439*, 305.
17. Bowman, S.; Hu, X.; Jiang, Q.; Qiu, Y.; Liu, W.; Wei, Y. *Coatings*. **2018**, *8*, 149.
18. Gargano, A.; Pingkarawat, K.; Pickerd, V. L.; Ibrahim, M. E.; Mouritz, A. P. *Compos. Sci. Technol.* **2017**, *138*, 68.
19. Sandler, J.; Werner, P.; Shaffer, M. S.; Demchuk, V.; Altstädt, V.; Windle, A. H. *Compos. Part A: Appl. Sci. Manuf.* **2002**, *33*, 1033.
20. Veazey, D.; Hsu, T.; Gomez, E. D. *J. Appl. Polym. Sci.* **2017**, *134*, 44441.
21. Ghaseminejhad, M. N.; Parvizi-Majidi, A. *Construct. Build Mater.* **1990**, *4*, 194.
22. Pimenta, S.; Pinho, S. T. *Waste Manag.* **2011**, *31*, 378.
23. Yang, Y.; Boom, R.; Irion, B.; van Heerden, D. J.; Kuiper, P.; de Wit, H. *Chem. Eng. Process. Process Intensif.* **2012**, *51*, 53.
24. Asmatulu, E.; Twomey, J.; Overcash, M. *J. Compos. Mater.* **2014**, *48*, 593.
25. Ma, Y., Kim, D., Williams, T. J., Nutt, S. R. In Proceedings of the 2017 Society for the Advancement of Material and Process Engineering (SAMPE) Technical Conference; Seattle, WA **2017**.
26. Kemmish, D. Update on the Technology and Applications of Polyaryletherketones; iSmithers: Shropshire, **2010**.
27. Duchoslav, J.; Unterweger, C.; Steinberger, R.; Fürst, C.; Stifter, D. *Polym. Degrad. Stab.* **2016**, *125*, 33.
28. Giraud, I.; Franceschi-Messant, S.; Perez, E.; Lacabanne, C.; Dantras, E. *Appl. Surf. Sci.* **2013**, *266*, 94.
29. Giraud, I.; Franceschi, S.; Perez, E.; Lacabanne, C.; Dantras, E. *J. Appl. Polym. Sci.* **2015**, *132*, 42550.
30. Chen, J.; Wang, K.; Zhao, Y. *Compos. Sci. Technol.* **2018**, *154*, 175.

31. Crevecoeur, G.; Groeninckx, G. *Macromolecules*. **1991**, *24*, 1190.
32. Lustig, S. R.; Van Alsten, J. G.; Hsiao, B. *Macromolecules*. **1993**, *26*, 3885.
33. Hsiao, B. S.; Sauer, B. B. *J. Polym. Sci. Part B: Polym. Phys.* **1993**, *31*, 901.
34. Shibata, M.; Fang, Z.; Yosomiya, R. *J. Appl. Polym. Sci.* **2001**, *80*, 769.
35. Buggy, M.; O'Byrne, K. *J. Appl. Polym. Sci.* **1997**, *65*, 2025.
36. Mitschang, P.; Blinzler, M.; Wöginger, A. *Compos. Sci. Technol.* **2003**, *63*, 2099.
37. Tan, W.; Falzon, B. G. *Compos. Sci. Technol.* **2016**, *126*, 60.
38. Alexandre, M.; Perez, E.; Lacabanne, C.; Dantras, E.; Franceschi, S.; Coudeyre, D.; Garrigues, J.-C. *Adv. Mater.* **2018**, *7*, 118.
39. Zhang, S. W. *Tribol. Int.* **1998**, *31*, 49.
40. Schön, J. *Wear*. **2004**, *257*, 395.
41. Bessaguet, C.; Dantras, E.; Lacabanne, C.; Chevalier, M.; Michon, G. *J. Non Cryst. Solids*. **2017**, *459*, 83.